

Emergent limits of an indirect measurement from phase transitions of inference

Satoru Tokuda,^{1,2,*} Kenji Nagata,² and Masato Okada^{2,3}

¹*Mathematics for Advanced Materials – Open Innovation Laboratory,
AIST, c/o Advanced Institute for Materials Research,
Tohoku University, Sendai, Miyagi, 980-8577, Japan*

²*Department of Complexity Science and Engineering,
The University of Tokyo, Kashiwa, Chiba 277-8561, Japan*

³*Center for Materials Research by Information Integration,
National Institute for Materials Science, Tsukuba, Ibaraki 305-0047, Japan*

(Dated: January 7, 2020)

Measurements are inseparable from inference, where the estimation of signals of interest from other observations is called an indirect measurement. While a variety of measurement limits have been defined by the physical constraint on each setup, the fundamental limit of an indirect measurement is essentially the limit of inference. Here, we propose the concept of statistical limits on indirect measurement: the bounds of distinction between signals and noise and between a signal and another signal. By developing the asymptotic theory of Bayesian regression, we investigate the phenomenology of a typical indirect measurement and demonstrate the existence of these limits. Based on the connection between inference and statistical physics, we also provide a unified interpretation in which these limits emerge from phase transitions of inference. Our results could pave the way for novel experimental design, enabling assess to the required quality of observations according to the assumed ground truth before the concerned indirect measurement is actually performed.

* s.tokuda@aist.go.jp

I. INTRODUCTION

Measurements are the foundation of science and engineering. Until recently, it had been implicitly believed that measurements are bounded only by physical constraints. But as it is, measurements are also inseparable from inference. The standard quantum limit had been regarded as a measurement limit. Some recent studies, however, showed that this limit can be surpassed, in terms of inference, by considering the quantum-mechanical nature of a photon, such as two-photon [1–5] and four-photon processes [6–8]. The diffraction limit had been regarded as a limit of an optical measurement. Some recent studies, however, showed that this limit can be surpassed, in terms of inference, by considering the kind of point spread function in the experiment [9–12].

The fundamental limit of an indirect measurement, which estimates signals of interest from other observations, is essentially the limit of inference. Compressed sensing involves an inference of sparse source signals from compressively mixed signals [13, 14]. Such an inference can surpass the Nyquist sampling rate, while it has a typical limit emerging from the *phase transition* of inference [15–20]. On the basis of the connection between statistical inference and statistical physics [21–24], it has been shown that many other high-dimensional statistical inferences, such as error-correcting codes [25], the perceptron [26], community detection [27, 28], and matrix factorization [29], also have typical limits emerging from phase transitions. Watanabe showed that there exist essentially the same phenomena as with phase transitions even in low-dimensional statistical inference and provided a new or different definition of phase transitions in statistical inference [30, 31].

In this study, we propose the concept of statistical limits for an indirect measurement. The statistical limits are classified into two types: bounds of distinction between signals and noise (signal detection limit, SDL) and between a signal and another signal (signal resolution limit, SRL). To demonstrate the existence of these limits, we investigate the phenomenology of a typical indirect measurement by developing the asymptotic theory of Bayesian regression with conditionally independent observations. From the perspective of statistical physics, we also provide a unified interpretation in which these limits emerge from phase transitions of inference and show the phase diagram described by the magnitude of the noise and degree of overlap between each signal.

II. RESULTS

A. Setup

We study an indirect measurement of source signals via mixed signals (Fig. 1). Suppose the set $\{\phi_k\}_{k=1}^K$ of K source signals, defined as a Gaussian function

$$\phi_k(x; \mu_k, \rho_k) := \exp\left(-\frac{\rho_k}{2}(x - \mu_k)^2\right) \quad (1)$$

with $x \in \mathbb{R}$, $\mu_k \in \mathbb{R}$, and $\rho_k \geq 0$. This type of unimodal source signal is ubiquitous in various fields, e.g., the spectral line shape in spectroscopy, pulse shape in electronics, and point spread function in optics.

The set of n mixed signals $\{Y_i\}_{i=1}^n$ with noise is observed as conditionally independent random variables subjected to the conditional probability density function

$$p(y_i | x_i, w, b) := \sqrt{\frac{b}{2\pi}} \exp\left(-\frac{b}{2}(y_i - f(x_i; w))^2\right) \quad (2)$$

with the observation noise variance $b^{-1} \geq 0$ and fixed observation points $x_i = x_{i-1} + \Delta x$ for $\Delta x := |x_n - x_1|/(n-1)$, where the superposition of K source signals is

$$f(x; w) := \sum_{k=1}^K a_k \phi_k(x; \mu_k, \rho_k) \quad (3)$$

with $a_k \geq 0$ in the parameter set $w := \{a_k, \rho_k, \mu_k\}_{k=1}^K$. Note that $f(x; w) = 0$ is defined for $K = 0$, which corresponds to the case of no source signal.

Suppose that $D^n := \{x_i, Y_i\}_{i=1}^n$ is a sample taken from $p(y_i | x_i, w_0, b_0)$ with the ground truth $w = w_0$, $K = K_0$ and $b = b_0$. In other words, the ground truth is unobservable while $D^n := \{x_i, Y_i\}_{i=1}^n$ is observable. It is considered that $\{\phi_k\}_{k=1}^{K_0}$ is indirectly observed by estimating w_0 , K_0 and b_0 from D^n . By means of Bayesian inversion, w_0 is

estimated as the posterior distribution

$$\begin{aligned} p(w \mid D^n, b, K) &= \frac{1}{p(D^n \mid b, K)} \prod_{i=1}^n p(Y_i \mid x_i, w, b) \varphi(w \mid K) \\ &\propto \exp\left(-\frac{nb}{2} E_n(w)\right) \varphi(w \mid K) \end{aligned} \quad (4)$$

with the mean square error

$$E_n(w) := \frac{1}{n} \sum_{i=1}^n (Y_i - f(x_i; w))^2, \quad (5)$$

where $\varphi(w \mid K)$ is some prior distribution and $p(D^n \mid b, K)$ is the marginal likelihood, with b and K as hyperparameters. This is a straightforward extension of the least squares method. In the same manner as in our previous work [32], b_0 and K_0 are estimated by maximizing $p(D^n \mid b, K)$ or, equivalently, by minimizing the function $\tilde{F}_n(b, K) := -\log p(D^n \mid b, K)$, which is called the Bayes free energy.

B. Self-averaging property

There are two kinds of random variables $\{Y_i\}_{i=1}^n$ and w in our setup. We first consider the typicality of our setup, which is independent of the realization of $\{Y_i\}_{i=1}^n$, by means of the conditional expectation over $\{Y_i\}_{i=1}^n \mid \{x_i\}_{i=1}^n$: $[\cdots] := \int(\cdots) \prod_{i=1}^n p(y_i \mid x_i, w_0, b_0) dy_i$. We derived the relation

$$E_n(w) = [E_n(w)] + O_p\left(\frac{1}{\sqrt{nb_0}}\right) \quad (6)$$

with

$$[E_n(w)] = \frac{1}{b_0} + \frac{1}{n} \sum_{i=1}^n (f(x_i; w_0) - f(x_i; w))^2. \quad (7)$$

This relation means that $E_n(w) = [E_n(w)]$ holds for $n \rightarrow \infty$. This property is called self-averaging, which is the concept originally proposed in the field of statistical physics of disordered systems [33]. In practice, it is difficult to ignore the term $O_p((\sqrt{nb_0})^{-1})$ as $b_0 \ll 1$, i.e., as the observation is too noisy. Notably, $[E_n(w_0)] = b_0^{-1}$ always holds, and $[E_n(w_0)] = 0$ especially holds for $b_0 \rightarrow \infty$ as the noiseless limit.

We also proved that $\tilde{F}_n(b, K)$ is self-averaging; i.e., $\tilde{F}_n(b, K) = [\tilde{F}_n(b, K)]$ holds for $n \rightarrow \infty$. This self-averaging property is precisely given by the asymptotic form

$$\tilde{F}_n(b, K) = b' \tilde{F}(b', K; w_0) - \frac{n}{2} \log \frac{b}{2\pi} + \frac{bR_n}{2b_0} \quad (8)$$

with

$$\tilde{F}(b', K; w_0) := -\frac{1}{b'} \log \int \exp\left(-\frac{b'}{2} H(w; w_0)\right) \varphi(w \mid K) dw \quad (9)$$

for $b' := b/\Delta x$ as the inverse of the *effective* noise variance and the Riemann integral

$$H(w; w_0) := \int_{x_1}^{x_n} (f(x; w_0) - f(x; w))^2 dx, \quad (10)$$

where R_n is a random variable following the chi-square distribution with n degree of freedom; $R_n \rightarrow n$ holds for $n \rightarrow \infty$, while $[R_n] = n$ always holds. Note that $H(w; w_0)$ can be expressed more explicitly (see Supplementary note 1). In the sense of a saddle point approximation for $w = w_0$ as $n \rightarrow \infty$, we obtain $\tilde{F}(b', K_0; w_0) = 0$ for $\varphi(w_0 \mid K_0) > 0$. Then, $b = b_0$ is a stationary point of $\tilde{F}_n(b, K_0)$. This means that b minimizing $\tilde{F}_n(b, K_0)$ converges to b_0 as $n \rightarrow \infty$; i.e., the estimator of b is consistent.

We should mention that K minimizing $\tilde{F}(b', K; w_0)$ is equal to K minimizing $\tilde{F}_n(b, K)$ when b is fixed. There can be a point at the intersection of $\tilde{F}(b', K; w_0)$ with $\tilde{F}(b', K'; w_0)$ for $K \neq K'$; a phase transition of statistical inference can occur with a variation in b' . Note that $\tilde{F}(b', K'; w_0)$ enables us to access the typicality of such a phenomenon, which is independent of the realization of $\{Y_i\}_{i=1}^n$ for $n \rightarrow \infty$.

C. Bayes specific heat

We quantify a kind of fluctuation in the indirect measurement of w via D^n by means of the conditional expectation over $w \mid D^n$: $\langle \cdots \rangle := \int (\cdots) p(w \mid D^n, b, K) dw$. We introduced the Bayes specific heat, a quantity characterizing the *phase* of statistical inference:

$$\tilde{C}_n(b, K) = \left(\frac{nb}{2} \right)^2 (\langle E_n(w)^2 \rangle - \langle E_n(w) \rangle^2). \quad (11)$$

Note that Eq. (11) is derived from our general definition of the Bayes specific heat in statistical inference (see Supplementary note 2).

We proved that $\tilde{C}_n(b, K) = [\tilde{C}_n(b)]$ holds especially for $n \rightarrow \infty$ with $b = O(b_0/\log n)$; i.e., $\tilde{C}_n(b, K)$ is conditionally self-averaging. This conditionally self-averaging property is precisely given by the finite-size scaling relation

$$\tilde{C}_n(b, K) = \Lambda(b', K; w_0) + O_p \left(\max \left(\frac{1}{\log nb}, \frac{b}{b_0}, \frac{1}{n\sqrt{b_0}} \right) \right) \quad (12)$$

with the scaling function

$$\Lambda(b', K; w_0) := \left(\frac{b'}{2} \right)^2 (\langle H(w; w_0)^2 \rangle - \langle H(w; w_0) \rangle^2). \quad (13)$$

Note that Eq. (12) means that the bivariate function of (n, b) is effectively reduced to the univariate function of b' for $n \rightarrow \infty$ with $b = O(b_0/\log n)$. The quantity $\tilde{C}_n(b, K)$ is not necessarily self-averaging under the condition $b = b_0$, corresponding to the Nishimori line [34, 35]; i.e., $\tilde{C}_n(b_0, K) = \Lambda(b_0/\Delta x, K; w_0) + O_p(1)$ holds. In practice, it is difficult to ignore the term $O_p((n\sqrt{b_0})^{-1})$ as $b_0 \ll 1$, i.e., as the observation is too noisy.

There is a remarkable junction between our physical insight and Watanabe's theory of statistical inference [31, 36–41]. The value of $\Lambda(b', K; w_0) \geq 0$ is known as a birational invariant, called the real log canonical threshold, in Watanabe's theory and originally in the fields of algebraic geometry and algebraic analysis [42–45]. The equation $2\Lambda(b', K; w_0) = 3K$ holds if $p(w \mid D^n, b, K)$ is sufficiently approximated by a Gaussian distribution (regular case) [31, 36–38].

We should mention that $\Lambda(b', K; w_0)$ enables us to characterize the typical phase of statistical inference, which is independent of the realization of $\{Y_i\}_{i=1}^n$ for $n \rightarrow \infty$, while Eq. (12) means that $\Lambda(b', K; w_0)$ is surely observable only for $b = O(b_0/\log n)$. This constraint is related to Watanabe's corollary [41], while the difference between the noise variance and *temperature* should also be considered (see Supplementary notes 2 and 3).

D. Signal detection limit

Here, we show a paradigmatic example of the SDL. Suppose that one source signal constitutes the ground truth (Fig. 2a), i.e., $f(x_i; w_0) = a_1 \phi_1(x; \mu_1, \rho_1)$ and that the mixed signals, i.e., some realization of D^n , are obtained in the presence of observation noise of some magnitude. If the magnitude of the noise is large enough, no signals can be detected (Fig. 2b). If the magnitude of the noise is small enough, the source signal is successfully detected (Fig. 2c). These results are actually demonstrated by performing a Monte Carlo (MC) simulation (see Methods section) and imply the existence of an SDL as a critical magnitude of the noise, which specifies whether or not the source signal is detectable.

To elucidate that there typically exists an SDL, which is independent of the realization of $\{Y_i\}_{i=1}^n$, we calculated $\tilde{F}(b', K; w_0)$ and $\Lambda(b', K; w_0)$ for w_0 of the above example. Phenomenologically, the value of K that minimizes $\tilde{F}(b', K; w_0)$ changes from 0 to 1 around $b' = b'_{\text{sn}}$ (Fig. 3a), while $\Lambda(b', 1; w_0)$ has a peak around $b' = b'_{\text{sn}}$ (Fig. 3b); there is a phase transition of statistical inference, and b'_{sn} corresponds to the SDL. The magnitudes of the noise in the cases of Fig. 2a and Fig. 2b correspond to $b' = b'_1$ and $b' = b'_2$ (Fig. 3); these cases are in different phases, and there exists an SDL as the boundary between these phases under the condition $b = b_0$.

This phase transition is also understandable as a variation in the posterior distribution (Fig. 4). While $p(w \mid D^n, b, 1)$ at $b' = b'_1$ (Fig. 4a-4c) is fairly consistent with $\varphi(w \mid 1)$, $p(w \mid D^n, b, 1)$ at $b' = b'_2$ is sufficiently approximated by a Gaussian distribution with mean w_0 (Fig. 4g-4i). In addition, $p(w \mid D^n, b, 1)$ at $b' = b'_{\text{sn}}$ represents the intermediate state (Fig. 4d-4f) between these two states. Correspondingly, $\Lambda(b', 1; w_0)$ is fairly consistent with 0 and $1.5 (= 3K_0/2)$ at $b' \ll b'_{\text{sn}}$ and $b' \gg b'_{\text{sn}}$, respectively (Fig. 3b); the case of $K = 1$ is regular at $b' = b'_2$.

We should mention that this phenomenon is essentially the same as, but slightly different from, the phenomenon called freeze-out [46]. Freeze-out was investigated only in the case where the sample is independently and identically

distributed; our setup corresponds to the conditionally independent case, where the self-averaging property needs to be considered. Freeze-out occurs with a variation in the sample size, which is generally different from the magnitude of the noise. One of our contributions in terms of the general aspect of statistical inference is the derivation of Eq. (12), i.e., the finite-size scaling relation between the sample size and magnitude of the noise. In a strict sense, finite-size effects should also be considered (see Supplementary note 3).

E. Signal resolution limit

Here, we show a paradigmatic example of the SRL. Suppose that two strongly overlapping source signals constitute the ground truth, i.e., $f(x_i; w_0) = a_1\phi_1(x; \mu_1, \rho_1) + a_2\phi_2(x; \mu_2, \rho_2)$, which appears almost as one (Fig. 5a), and that the mixed signals, i.e., some realization of D^n , are obtained in the presence of observation noise of some magnitude. If the magnitude of the noise is large enough, one source signal is detected (Fig. 5b), which is statistically optimal but a misestimation of the ground truth. If the magnitude of noise is small enough, two source signals are successfully detected and resolved (Fig. 5c). These results are actually demonstrated by performing an MC simulation (see Methods section) and imply the existence of an SRL as the critical magnitude of the noise, which specifies whether or not the strongly overlapping source signals are resolvable.

To elucidate that there typically exists an SRL, which is independent of the realization of $\{Y_i\}_{i=1}^n$, we calculated $\tilde{F}(b', K; w_0)$ and $\Lambda(b', K; w_0)$ for w_0 of the above example. As in Sec. IID, the value of K that minimizes $\tilde{F}(b', K; w_0)$ changes from 0 to 1 around $b' = b'_{\text{sn}}$ (Fig. 6a), while $\Lambda(b', 1; w_0)$ has a peak around $b' = b'_{\text{sn}}$ (Fig. 6b); there is a phase transition of statistical inference, and b'_{sn} corresponds to the SDL. Unlike in Sec. IID, the value of K that minimizes $\tilde{F}(b', K; w_0)$ changes from 1 to 2 around $b' = b'_{\text{ss}}$ (Fig. 6a), while $\Lambda(b', 2; w_0)$ has a peak around $b' = b'_{\text{ss}}$ (Fig. 6b); there is another phase transition of statistical inference, and b'_{ss} corresponds to the SRL. The magnitudes of the noise in the cases of Fig. 5a and Fig. 5b correspond to $b' = b'_2$ and $b' = b'_3$ (Fig. 6); these cases are in different phases, and there exists an SRL as the boundary between these phases under the condition $b = b_0$.

This phase transition is also understandable as a variation in the posterior distribution (Fig. 7). While $p(w | D^n, b, 2)$ at $b' = b'_2$ (Fig. 7a-7c) is far from a Gaussian distribution, $p(w | D^n, b, 2)$ at $b' = b'_3$ is sufficiently approximated by a Gaussian distribution with mean w_0 (Fig. 7g-7i). In addition, $p(w | D^n, b, 2)$ at $b' = b'_{\text{ss}}$ represents the intermediate state (Fig. 7d-7f) between these two states. Correspondingly, $\Lambda(b', 2; w_0)$ is fairly consistent with $1.5(= \Lambda(b', 1; w_0))$ and $3(= 3K_0/2)$ at $b'_{\text{sn}} \ll b' \ll b'_{\text{ss}}$ and $b' \gg b'_{\text{ss}}$, respectively (Fig. 6b); the case of $K = 2$ is regular at $b' = b'_3$.

We should explain why $p(w | D^n, b, 2)$ at $b' = b'_2$ (Fig. 7a-7c) exhibits such correlation in the parameters. Although the ground truth is w_0 with $K_0 = 2$, here, we consider the pseudo-ground truth $\tilde{w}_0 := \{\tilde{a}_0, \tilde{\rho}_0, \tilde{\mu}_0\}$ with $\tilde{K}_0 = 1$ and the analytic set

$$\begin{aligned} \tilde{W}_0 &:= \{w \mid f(x_i; w) = f(x_i; \tilde{w}_0)\} \\ &= \tilde{W}_{01} \cup \tilde{W}_{02} \cup \tilde{W}_{03} \end{aligned} \quad (14)$$

of w with $K = 2$, where

$$\tilde{W}_{01} := \{w \mid a_k + a_{k'} = \tilde{a}_0, \rho_k = \rho_{k'} = \tilde{\rho}_0, \mu_k = \mu_{k'} = \tilde{\mu}_0\},$$

$$\tilde{W}_{02} := \{w \mid a_k = \tilde{a}_0, a_{k'} = 0, \rho_k = \tilde{\rho}_0, \mu_k = \tilde{\mu}_0\}$$

and

$$\tilde{W}_{03} := \{w \mid a_k = \tilde{a}_0, \rho_k = \tilde{\rho}_0, \mu_k = \tilde{\mu}_0, \phi_{k'}(x_i; \mu_{k'}, \rho_{k'}) = 0\}$$

for $i = 1, \dots, n$ and $k \neq k'$. Note that $\phi_{k'}(x_i; \mu_{k'}, \rho_{k'}) = 0$ holds for $\rho_{k'} \rightarrow \infty$ or $\mu_{k'} \rightarrow \pm\infty$, where $\rho_{k'} \neq 0$ and $\mu_{k'} \neq x_i$ are necessary. Notably, $H(\tilde{w}; \tilde{w}_0) = 0$ holds for $\forall \tilde{w} \in \tilde{W}_0$; i.e., $p(w | D^n, b, 2)$ can be relatively large around $w = \tilde{w}$ for $\varphi(w | 2) > 0$. The above scenario of the pseudo-ground truth corresponds to $p(w | D^n, b, 2)$ at $b' = b'_2$ (Fig. 7a-7c); i.e., $w \simeq \tilde{w}_0$ is statistically optimal for the case of $K = 2$ at $b' = b'_2$. This scenario qualitatively holds at any $b'_{\text{sn}} \ll b' \ll b'_{\text{ss}}$, since $\Lambda(b', 2; w_0)$ is fairly consistent with $1.5(= \Lambda(b', 1; w_0))$. Note that this result is from the situation where $f(x_i; w_0) = a_1\phi_1(x; \mu_1, \rho_1) + a_2\phi_2(x; \mu_2, \rho_2)$ appears almost as one signal (Fig. 5a), where a crucial problem is implied in the context of spectroscopic measurements [32]; there is a risk of failure to recognize whether or not an energy level is degenerate.

F. Phase diagram

We also investigated the dependence of the phase of indirect measurements on the degree of overlap between each signal. We introduce $\delta := |\mu_1^* - \mu_2^*|/2$, defined by $w_0 = \{a_k^*, \rho_k^*, \mu_k^*\}_{k=1}^{K_0}$ with $K_0 = 2$, as the degree of overlap between $\phi_1(x; \mu_1^*, \rho_1^*)$ and $\phi_2(x; \mu_2^*, \rho_2^*)$. Note that w_0 is same as the setting of Fig. 5a except for μ_1^* and μ_2^* .

The phase diagram shows that there are three phases described by b' and δ (Fig. 8). The boundaries corresponding to $\tilde{F}(b', 0; w_0) = \tilde{F}(b', 1; w_0)$ and $\tilde{F}(b', 1; w_0) = \tilde{F}(b', 2; w_0)$ are the SDL and SRL, respectively, under the condition $b = b_0$; the SRL is always a tighter bound than the SDL. There is a clear dependence such that the smaller δ is, the larger the critical b' as the SRL. We should mention that the cases of Secs. IID and IIE correspond to $\delta = 0$ and $\delta = 0.25$, respectively; the case of $\delta = 0$ is essentially regarded as $K_0 = 1$, while the ground truth is surely $K_0 = 2$. In other words, there exists \tilde{w}_0 that satisfies $f(x; w_0) = f(x; \tilde{w}_0)$ in the case of $\delta = 0$ even if $w_0 \neq \tilde{w}_0$. This situation corresponds to the *nonidentifiable* case in Watanabe's theory [38], where $\delta = 0$ is a singularity, and $\delta > 0$ corresponds to a distance from the singularity as mentioned by Watanabe and Amari [47]. Note that there are only two phases at $\delta = 0$; the SRL does not emerge.

We should mention the relation between the peak positions of $\Lambda(b', 2; w_0)$ and the SDL and SRL. In Secs. IID and IIE, the phase of statistical inference was defined by K minimizing $\tilde{F}(b', K; w_0)$ and was characterized by $\Lambda(b', K; w_0)$. Here, we consider this chicken or egg problem more precisely. First, $\tilde{F}(b', K; w_0)$ relatively characterizes a phase of statistical inference by comparing $\tilde{F}(b', K'; w_0)$ with $K \neq K'$, while $\Lambda(b', K; w_0)$ absolutely characterizes the phase. In other words, the former approach monitors the state of the hyperparameter optimization or model selection, while the latter approach monitors the state of the parameter estimation. In the latter approach, it can be said that there are only two phases at $\delta \gtrsim 1$, where the two peak positions of $\Lambda(b', 2; w_0)$ merge. If two source signals are detectable, then they are also resolvable at the same time. In the region bounded by the SDL, the SRL, and $\delta \gtrsim 1$, $K = 1$ is statistically optimal, but w is not sufficiently estimated; i.e., $p(w | D^n, b, 1)$ is far from a Gaussian distribution. From this viewpoint, the peak positions of $\Lambda(b', 2; w_0)$ can be regarded as a tighter bound than the SDL and SRL under the condition $b = b_0$.

III. DISCUSSION

Our results can be utilized for experimental design in the form of *virtual measurement analytics* [48]; we can virtually check the noise immunity of an arbitrary indirect measurement by following our procedure. In other words, we can preliminarily consider the typically required quality of observations, i.e., $b_0/\Delta x$ beyond the SDL and SRL, by emulating the indirect measurement with the assumed ground truth w_0 before the concerned measurement is actually performed. Note that our procedure can be applied to not only a Gaussian signal ϕ_k but also any type of source signal without loss of generality.

Our results also contribute to the development of some new aspects of statistical inference. The results in Sec. IIB can be regarded as a frontier of the asymptotic theory of the regression problem with conditionally independent observations. The point is that Eqs. (6-13) always hold without loss of generality, even if $f(x; w)$ is replaced by any other regression function. This means that the self-averaging property has not been argued enough at least in the context of Watanabe's theory [31]. The results in Sec. IIC can be regarded as a frontier of statistical inference with a broader meaning. The definition of the Bayes specific heat and the derivation of Eq. (11) are different from the quantity called the learning capacity [46] (see Supplementary notes 2 and 3). Our definition and derivation reflect the consequence of Eqs. (12,13); the limits $n \rightarrow \infty$, $b \rightarrow \infty$ and $b_0 \rightarrow \infty$ are different.

It should be emphasized that we assumed the large-size limit $n \rightarrow \infty$ of the sample but did not take the high-dimension limit $\dim(w) \rightarrow \infty$ of the parameter into account. This situation is different from the ordinary picture of physics; the phase transitions shown in Secs. IID-IIF are outside the Ehrenfest classification but inside Watanabe's definition [31]. On the other hand, high-dimensional statistical inference as the limit $n, \dim(w) \rightarrow \infty$ such that $n/\dim(w)$ stays finite has been energetically studied [24–29]. In this case, there exist phase transitions characterized by the Ehrenfest classification. The first-order phase transitions, associated with metastability, are related to algorithmic hardness [24, 27–29, 49, 50]. Further studies can be pursued at the junction of our viewpoint and algorithmic hardness.

Our results are also related to machine learning. As Watanabe showed [31, 38], the generalization loss is associated with $\Lambda(b', K; w_0)$. This means that a drastic change in $\Lambda(b', K; w_0)$, i.e., a phase transition of inference, causes a qualitative change in the generalization performance. The widely applicable information criterion (WAIC) [39, 40], as a criterion for the generalization loss, is meaningful, while the cross-validation loss is meaningless since our setup is based on conditionally independent observations [31, 51]. The point is that the generalization loss and WAIC are not self-averaging, while $\tilde{F}_n(b, K)$ is self-averaging. From this viewpoint, our procedure may provide a perspective for the assessment of the typical generalization performance, which is independent of the realization of $\{Y_i\}_{i=1}^n$ for $n \rightarrow \infty$.

However, we must consider the difference between an indirect measurement and machine learning; their purposes, i.e., inference and prediction, are essentially different.

IV. METHODS

A. Outline of the derivation of Eq. (6)

Here, we show an outline of the derivation of Eq. (6). The average $[E_n(w)]$ (Eq. (7)) and the variance $[E_n(w)^2] - [E_n(w)]^2 = \frac{4}{n^2 b_0} \sum_i (f(x_i; w_0) - f(x_i; w))^2$ were exactly obtained. The relation $[E_n(w)^2] - [E_n(w)]^2 = O((nb_0)^{-1})$ holds, where $\frac{1}{n} \sum_i (f(x_i; w_0) - f(x_i; w))^2 = H(w; w_0)$ for $n \rightarrow \infty$. Then, we obtained Eq. (6).

B. Outline of the derivation of Eq. (8)

Here, we show an outline of the derivation of Eq. (8). By considering the noise additivity, we divided Y_i into the signal and noise, i.e., $Y_i = f(x_i; w_0) + N_i$, where $N_i \sim \mathcal{N}(0, b_0^{-1})$. Then, we obtained $nE_n(w) = \sum_i s_i(w)^2 + 2 \sum_i s_i(w)N_i + R_n/b_0$, where $s_i(w) := f(x_i; w_0) - f(x_i; w)$ and $R_n := b_0 \sum_i N_i^2$. By using Jensen's inequality, $[-\log \int \exp(-\frac{b}{2} (\sum_i s_i(w)^2 + 2 \sum_i s_i(w)N_i)) \varphi(w | K) dw] \geq -\log \int \exp(-\frac{b}{2} \sum_i s_i(w)^2) \varphi(w | K) dw$ holds, where the equality holds when $\sum_i s_i(w)N_i = 0$, which is asymptotically satisfied for $n \rightarrow \infty$. Based on this asymptotic equality, Eq. (8) was obtained.

C. Outline of the derivation of Eq. (12)

Here, we show an outline of the derivation of Eq. (12), where the details are shown in Supplementary note 3. First, we obtained the asymptotic behaviour of the Bayes specific heat from the second derivative of the Bayes free energy, whose asymptotic form was obtained by Watanabe [31, 36–38]. As a result, we found that the Bayes specific heat is generally divided into two parts, the real log canonical threshold as the average and a fluctuation of order $O_p(1/\log n)$. Second, we considered the specifics of our setup. By considering the noise additivity, $\tilde{C}_n(b, K)$ was also divided into two parts, the average over and a fluctuation by D^n . We evaluated the order of the fluctuation part and found that there are the terms of orders $O_p(b/b_0)$ and $O_p((n\sqrt{b_0})^{-1})$. Finally, we combined the general result and specifics and obtained Eq. (12).

D. Monte Carlo simulation

In Secs. IID-IIF, we performed an MC simulation by using parallel tempering [52, 53] based on the Metropolis criterion. The variable b' was discretized as 400 points consisting of $b = 0$ and 399 logarithmically spaced points in the interval $[10^{-9}, 10^{11}]$. By sampling from $p(w | D^n, b, K) \propto \exp(-\frac{b'}{2} H(w; w_0)) \varphi(w | K)$ with $\varphi(w | K) = \prod_{k=1}^K \exp(-a_k/10 - \rho_k/10 - \mu_k^2/50)/(500\sqrt{2\pi})$, we calculated $\tilde{F}(b', K; w_0)$ and $\Lambda(b', K; w_0)$ at each point of $b' > 0$, where the total MC sweeps were 100,000 after the burn-in. Bridge sampling [54, 55] was used to calculate $\tilde{F}(b', K; w_0)$. The error bars of $\tilde{F}(b', K; w_0)$ and $\Lambda(b', K; w_0)$ were calculated by bootstrap resampling [56]. Especially in Figs. 2 and 5, we sampled from $p(w | D^n, b, K) \propto \exp(-\frac{nb}{2} E_n(w)) \varphi(w | K)$ with a realization of D^n and calculated $\tilde{F}_n(b, K)$ in the same manner as in our previous work [32].

ACKNOWLEDGMENTS

The authors are grateful to Chihiro H. Nakajima, Koji Hukushima, Kouki Yonaga, Masayuki Ohzeki, Shotaro Akaho, Sumio Watanabe, Tomoyuki Obuchi and Yoshiyuki Kabashima for valuable discussions. M.O. was supported by a Grant-in-Aid for Scientific Research on Innovative Areas (No. 25120009) from the Japan Society for the Promotion of Science, the "Materials Research by Information Integration" Initiative (MI2I) project of the Support Program for Starting Up Innovation Hub from the Japan Science and Technology Agency (JST), and the Council for Science, Technology and Innovation (CSTI), Cross-ministerial Strategic Innovation Promotion Program (SIP), "Structural Materials for Innovation" (Funding agency: JST).

AUTHOR CONTRIBUTION

S.T. and M.O. conceived the project and concrete setup. S.T. derived all the equations, performed all the numerical calculations, interpreted the results and wrote the manuscript. K.N. partially supervised the project. M.O. supervised the project.

-
- [1] J. Rarity, P. Tapster, E. Jakeman, T. Larchuk, R. Campos, M. Teich, and B. Saleh, Physical review letters **65**, 1348 (1990).
 - [2] A. Kuzmich and L. Mandel, Quantum and Semiclassical Optics: Journal of the European Optical Society Part B **10**, 493 (1998).
 - [3] E. Fonseca, C. Monken, and S. Pádua, Physical Review Letters **82**, 2868 (1999).
 - [4] K. Edamatsu, R. Shimizu, and T. Itoh, Physical review letters **89**, 213601 (2002).
 - [5] H. Eisenberg, J. Hodelin, G. Khoury, and D. Bouwmeester, Physical review letters **94**, 090502 (2005).
 - [6] T. Nagata, R. Okamoto, J. L. O'brien, K. Sasaki, and S. Takeuchi, Science **316**, 726 (2007).
 - [7] R. Okamoto, H. F. Hofmann, T. Nagata, J. L. O'Brien, K. Sasaki, and S. Takeuchi, New Journal of Physics **10**, 073033 (2008).
 - [8] G.-Y. Xiang, B. L. Higgins, D. Berry, H. M. Wiseman, and G. Pryde, Nature Photonics **5**, 43 (2011).
 - [9] T. A. Klar, S. Jakobs, M. Dyba, A. Egner, and S. W. Hell, Proceedings of the National Academy of Sciences **97**, 8206 (2000).
 - [10] M. G. Gustafsson, Proceedings of the National Academy of Sciences **102**, 13081 (2005).
 - [11] E. Betzig, G. H. Patterson, R. Sougrat, O. W. Lindwasser, S. Olenych, J. S. Bonifacino, M. W. Davidson, J. Lippincott-Schwartz, and H. F. Hess, Science **313**, 1642 (2006).
 - [12] Y. Ashida and M. Ueda, Physical review letters **115**, 095301 (2015).
 - [13] E. J. Candes and T. Tao, IEEE Transactions on Information Theory **52**, 5406 (2006).
 - [14] D. L. Donoho *et al.*, IEEE Transactions on information theory **52**, 1289 (2006).
 - [15] D. L. Donoho, Discrete & Computational Geometry **35**, 617 (2006).
 - [16] D. Donoho and J. Tanner, Philosophical Transactions of the Royal Society A: Mathematical, Physical and Engineering Sciences **367**, 4273 (2009).
 - [17] Y. Kabashima, T. Wadayama, and T. Tanaka, Journal of Statistical Mechanics: Theory and Experiment **2009**, L09003 (2009).
 - [18] D. L. Donoho, A. Maleki, and A. Montanari, Proceedings of the National Academy of Sciences **106**, 18914 (2009).
 - [19] S. Ganguli and H. Sompolinsky, Physical review letters **104**, 188701 (2010).
 - [20] F. Krzakala, M. Mézard, F. Sausset, Y. Sun, and L. Zdeborová, Journal of Statistical Mechanics: Theory and Experiment **2012**, P08009 (2012).
 - [21] E. T. Jaynes, Physical review **106**, 620 (1957).
 - [22] E. T. Jaynes, *Probability theory: The logic of science* (Cambridge university press, 2003).
 - [23] V. Balasubramanian, Neural computation **9**, 349 (1997).
 - [24] L. Zdeborová and F. Krzakala, Advances in Physics **65**, 453 (2016).
 - [25] N. Surlas, Nature **339**, 693 (1989).
 - [26] H. S. Seung, H. Sompolinsky, and N. Tishby, Physical review A **45**, 6056 (1992).
 - [27] A. Decelle, F. Krzakala, C. Moore, and L. Zdeborová, Physical Review Letters **107**, 065701 (2011).
 - [28] A. Decelle, F. Krzakala, C. Moore, and L. Zdeborová, Physical Review E **84**, 066106 (2011).
 - [29] Y. Kabashima, F. Krzakala, M. Mézard, A. Sakata, and L. Zdeborová, IEEE Transactions on information theory **62**, 4228 (2016).
 - [30] S. WATANABE, in *SEVENTH WORKSHOP ON INFORMATION THEORETIC METHODS IN SCIENCE AND ENGINEERING* (Citeseer, 2014) p. 27.
 - [31] S. Watanabe, *Mathematical theory of Bayesian statistics* (CRC Press, 2018).
 - [32] S. Tokuda, K. Nagata, and M. Okada, Journal of the Physical Society of Japan **86**, 024001 (2016).
 - [33] I. M. Lifshitz, Soviet Physics Uspekhi **7**, 549 (1965).
 - [34] H. Nishimori, Journal of Physics C: Solid State Physics **13**, 4071 (1980).
 - [35] Y. Iba, Journal of Physics A: Mathematical and General **32**, 3875 (1999).
 - [36] S. Watanabe, in *International Conference on Algorithmic Learning Theory* (Springer, 1999) pp. 39–50.
 - [37] S. Watanabe, Neural Computation **13**, 899 (2001).
 - [38] S. Watanabe, *Algebraic geometry and statistical learning theory*, Vol. 25 (Cambridge University Press, 2009).
 - [39] S. Watanabe, Neural Networks **23**, 20 (2010).
 - [40] S. Watanabe, Journal of Machine Learning Research **11**, 3571 (2010).
 - [41] S. Watanabe, Journal of Machine Learning Research **14**, 867 (2013).
 - [42] I. Bernshtein, Functional Analysis and its applications **6**, 273 (1972).
 - [43] M. Sato and T. Shintani, Annals of Mathematics , 131 (1974).
 - [44] M. Kashiwara, Inventiones mathematicae **38**, 33 (1976).

- [45] A. N. Varchenko, Functional analysis and its applications **10**, 175 (1976).
- [46] C. H. LaMont and P. A. Wiggins, Physical Review E **99**, 052140 (2019).
- [47] S. Watanabe and S.-i. Amari, Neural Computation **15**, 1013 (2003).
- [48] K. Nagata, R. Muraoka, Y.-i. Mototake, T. Sasaki, and M. Okada, Journal of the Physical Society of Japan **88**, 044003 (2019).
- [49] F. Antenucci, S. Franz, P. Urbani, and L. Zdeborová, Physical Review X **9**, 011020 (2019).
- [50] F. Ricci-Tersenghi, G. Semerjian, and L. Zdeborová, Physical Review E **99**, 042109 (2019).
- [51] S. WATANABE, in *TENTH WORKSHOP ON INFORMATION THEORETIC METHODS IN SCIENCE AND ENGINEERING* (2017) p. 38.
- [52] C. J. Geyer, (1991).
- [53] K. Hukushima and K. Nemoto, Journal of the Physical Society of Japan **65**, 1604 (1996).
- [54] X.-L. Meng and W. H. Wong, Statistica Sinica , 831 (1996).
- [55] A. Gelman and X.-L. Meng, Statistical science , 163 (1998).
- [56] B. Efron *et al.*, The Annals of Statistics **7**, 1 (1979).

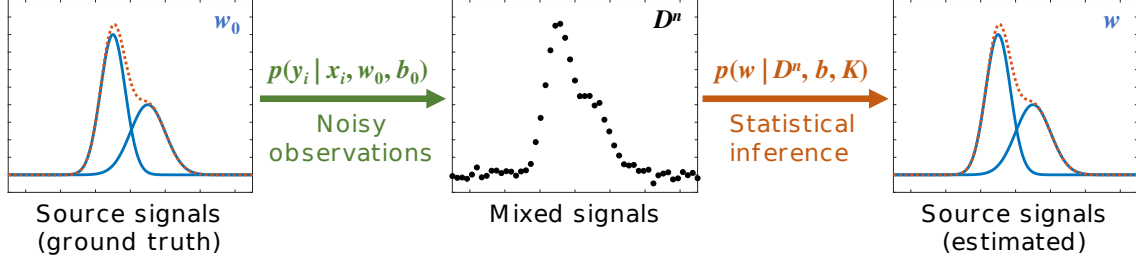


FIG. 1. Schematic of our setup. Mixed signals $D^n := \{x_i, Y_i\}_{i=1}^n$ (black dots), i.e., discretized $f(x_i; w_0)$ (red dotted line) as a superposition of $\{\phi_k\}_{k=1}^K$ (blue solid lines) with statistical noise, are taken from the conditional probability density function $p(y_i | x_i, w_0, b_0)$, where w_0 and b_0^{-1} are the ground truth of the parameter set and noise variance, respectively. Inversely, $\{\phi_k\}_{k=1}^K$ are estimated from D^n in the form of the parameter set w taken from the posterior distribution $p(w | D^n, b, K)$. The indirect measurement in our setup consists of these two processes. The problem here is that this indirect measurement is not always successfully performed due to the presence of statistical noise as with noisy-channel coding; the SDL and SRL typically exist.

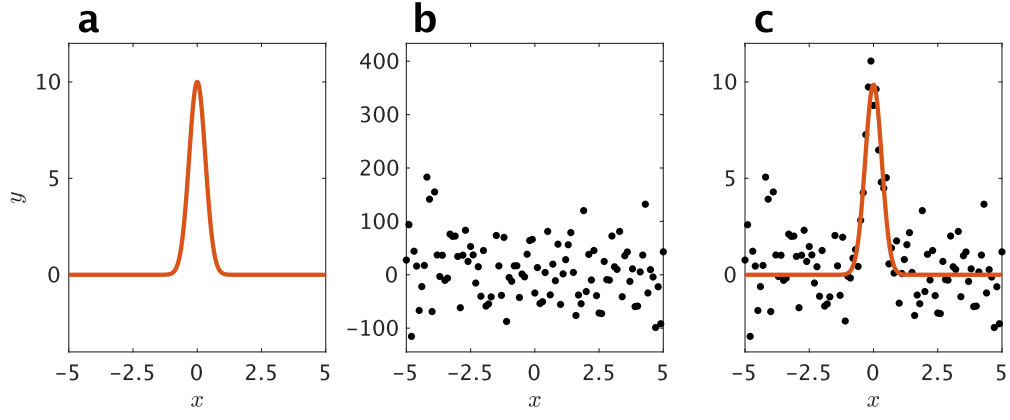


FIG. 2. Paradigmatic example of the signal detection limit. (a) Ground truth $f(x; w_0)$ (red line) with $w_0 = \{10, 10, 0\}$ as the $K_0 = 1$ source signal. (b) A realization of D^n (black dots) at $b_0 = b'_1 \Delta x$ for $n = 101$. It was simulated that $K = 0$ minimizes $\tilde{F}_n(b, K)$ for this D^n . (c) A realization of D^n (black dots) at $b_0 = b'_2 \Delta x$ for $n = 101$ and $f(x; \hat{w})$ (red line) with the maximum a posteriori (MAP) estimator \hat{w} . It was simulated that $K = 1$ minimizes $\tilde{F}_n(b, K)$ for this D^n .

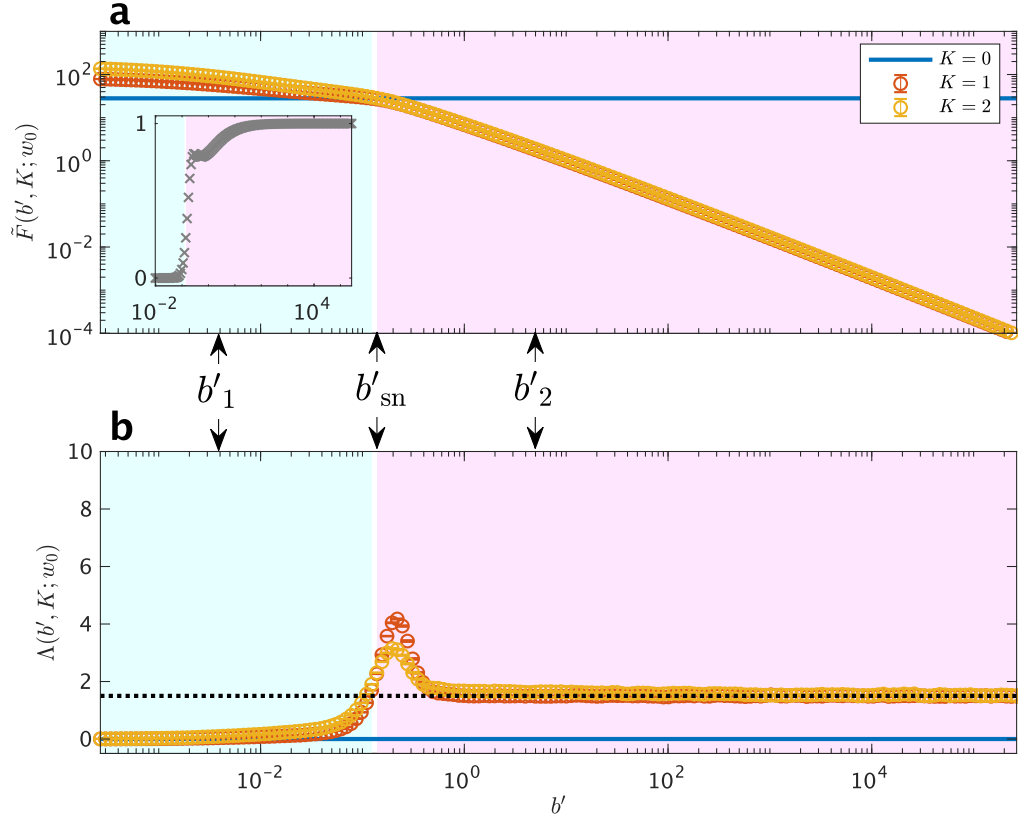


FIG. 3. Emergence of the signal detection limit as a phase boundary of statistical inference. **(a)** Log-log plot of $\tilde{F}(b', K; w_0)$ with $w_0 = \{10, 10, 0\}$ for $K_0 = 1$. The inequality $\tilde{F}(b', 0; w_0) < \tilde{F}(b', 1; w_0)$ holds for $b' < b'_{\text{sn}}$ (region in light blue), and $\tilde{F}(b', 0; w_0) > \tilde{F}(b', 1; w_0)$ holds for $b' > b'_{\text{sn}}$ (region in light pink). The Bayes factor $\exp(-b'(\tilde{F}(b', 2; w_0) - \tilde{F}(b', 1; w_0))) < 1$ holds for any b' (inset). **(b)** Semi-log plot of $\Lambda(b', K; w_0)$ with $w_0 = \{10, 10, 0\}$ for $K_0 = 1$ and asymptote $3K_0/2$ (black dotted line).

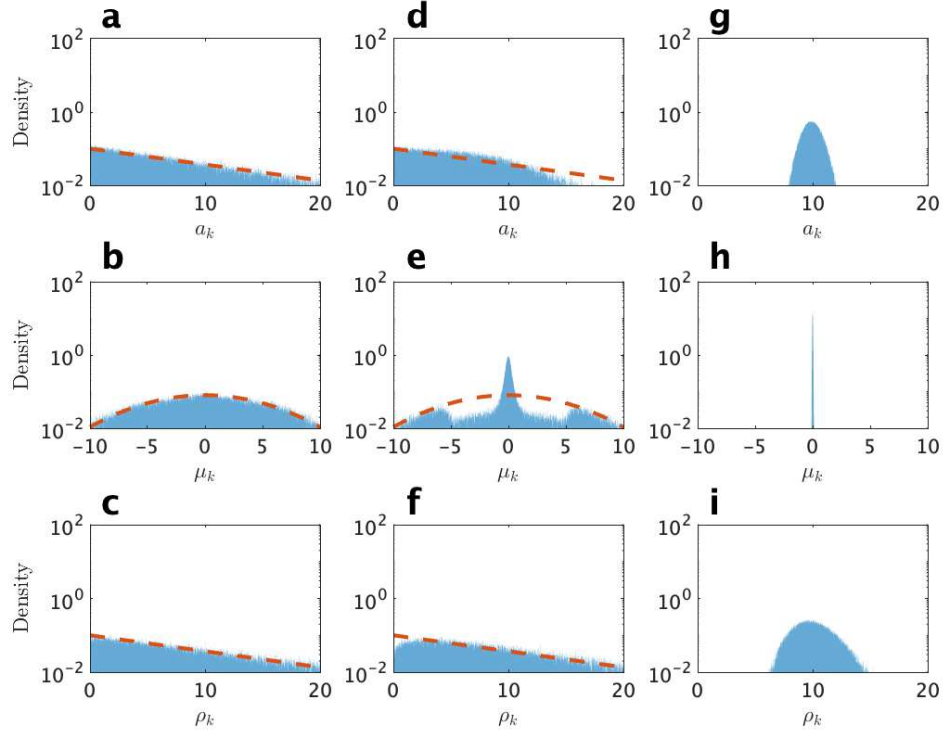


FIG. 4. Variation in the posterior distribution from the prior distribution with magnitude of the noise. Histogram of the MC sample from $p(w | D^n, b, 1) \propto \exp(-\frac{b'}{2}H(w; w_0))\varphi(w | K)$ with $w_0 = \{10, 10, 0\}$ for $K_0 = 1$ at (a-c) $b' = b'_1$, (d-f) $b' = b'_{sn}$, and (g-i) $b' = b'_2$. Each row corresponds to a marginal distribution; (a, d, g) corresponds to $p(a_1 | D^n, b, 1)$, (b, e, h) corresponds to $p(\mu_1 | D^n, b, 1)$, and (c, f, i) corresponds to $p(\rho_1 | D^n, b, 1)$. Compare each histogram with the marginal distribution of $\varphi(w | 1)$ (red dashed line).

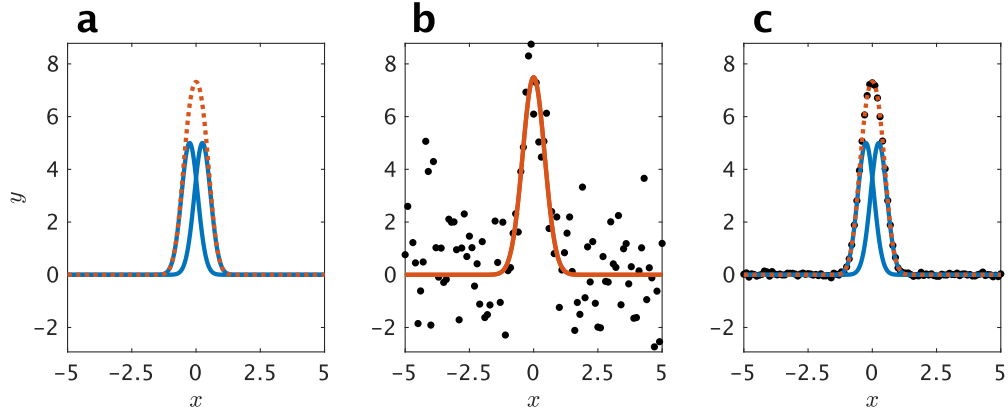


FIG. 5. Paradigmatic example of the signal resolution limit. (a) Ground truth $f(x; w_0)$ (red dotted line) with $w_0 = \{5, 10, \pm 0.25\}$ as a superposition of $K_0 = 2$ overlapping source signals (blue solid lines). (b) A realization of D^n (black dots) at $b_0 = b'_2 \Delta x$ for $n = 101$ and $f(x; \hat{w})$ (red solid line) with the MAP estimator \hat{w} . It was simulated that $K = 1$ minimizes $\tilde{F}_n(b, K)$ for this D^n . (c) A realization of D^n (black dots) at $b_0 = b'_3 \Delta x$ for $n = 101$ and $f(x; \hat{w})$ (red dotted line) with the MAP estimator \hat{w} as a superposition of two source signals (blue solid lines). It was simulated that $K = 2$ minimizes $\tilde{F}_n(b, K)$ for this D^n .

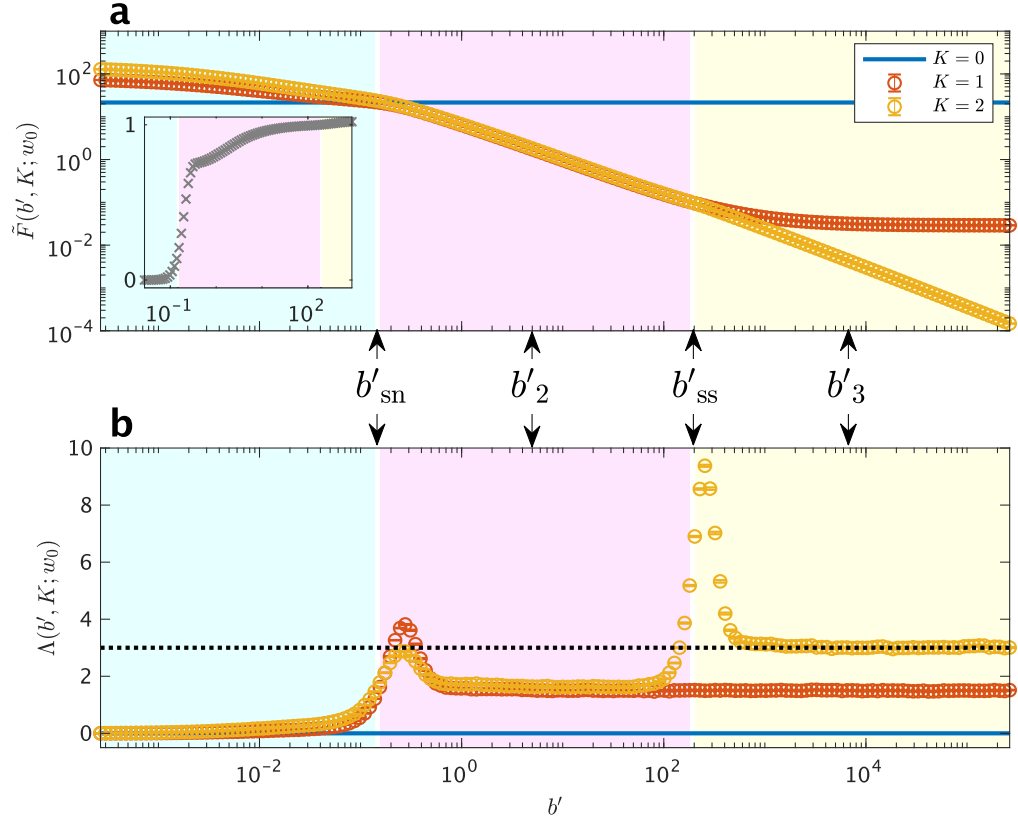


FIG. 6. Emergence of the signal resolution limit as a phase boundary of statistical inference. (a) Log-log plot of $\tilde{F}(b', K; w_0)$ with $w_0 = \{5, 10, \pm 0.25\}$ as $K_0 = 2$. The inequality $\tilde{F}(b', 0; w_0) < \tilde{F}(b', 1; w_0)$ holds for $b' < b'_{\text{sn}}$ (region in light blue), $\tilde{F}(b', 0; w_0) > \tilde{F}(b', 1; w_0)$ holds for $b'_{\text{sn}} < b' < b'_{\text{ss}}$ (region in light pink), and $\tilde{F}(b', 1; w_0) > \tilde{F}(b', 2; w_0)$ holds for $b' > b'_{\text{ss}}$ (region in light yellow). The Bayes factor $\exp(-b'(\tilde{F}(b', 2; w_0) - \tilde{F}(b', 1; w_0))) < 1$ holds for $b' < b'_{\text{ss}}$, and $\exp(-b'(\tilde{F}(b', 2; w_0) - \tilde{F}(b', 1; w_0))) > 1$ holds for $b' > b'_{\text{ss}}$ (inset). (b) Semi-log plot of $\Lambda(b', K; w_0)$ with $w_0 = \{5, 10, \pm 0.25\}$ and asymptote $3K_0/2$ (black dotted line).

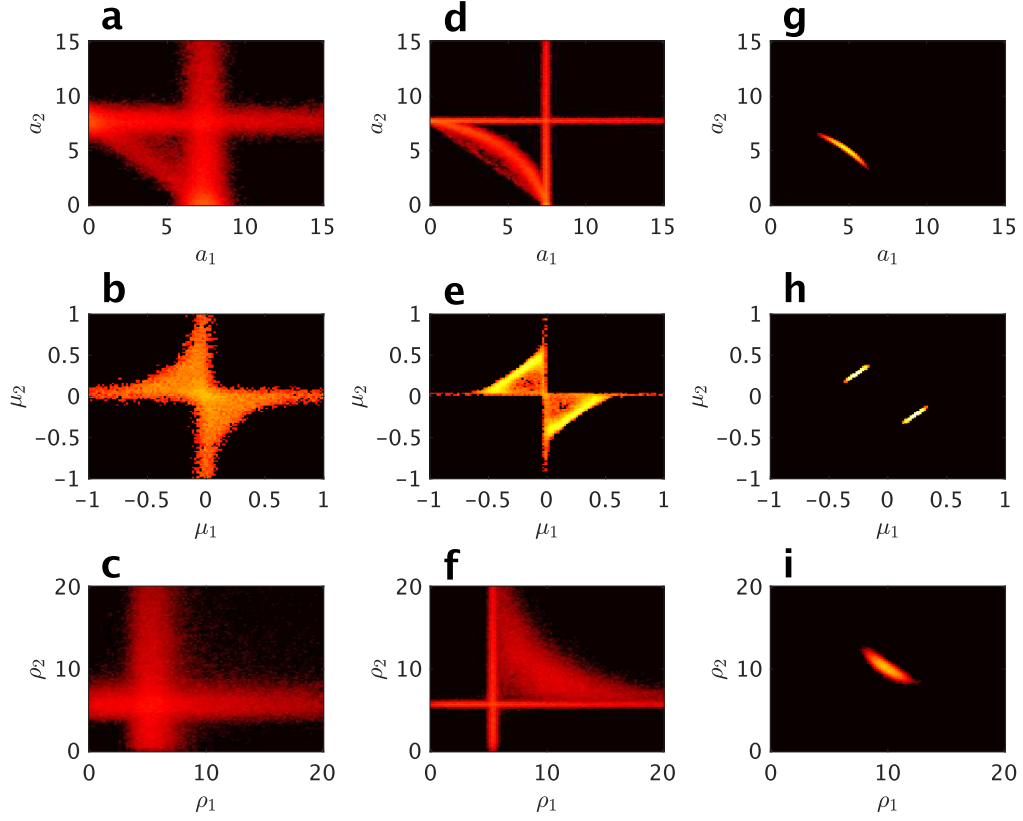


FIG. 7. Variation in the posterior distribution with the magnitude of the noise and underlying correlation of the parameters. Two-dimensional histogram of the MC sample from $p(w \mid D^n, b, 2) \propto \exp(-\frac{b'}{2}H(w; w_0))\varphi(w \mid K)$ with $w_0 = \{5, 10, \pm 0.25\}$ as $K_0 = 2$ at (a-c) $b' = b'_2$, (d-f) $b' = b'_{ss}$, and (g-i) $b' = b'_3$. Each row corresponds to a marginal distribution; (a, d, g) corresponds to $p(a_1, a_2 \mid D^n, b, 2)$, (b, e, h) corresponds to $p(\mu_1, \mu_2 \mid D^n, b, 2)$, and (c, f, i) corresponds to $p(\rho_1, \rho_2 \mid D^n, b, 2)$.

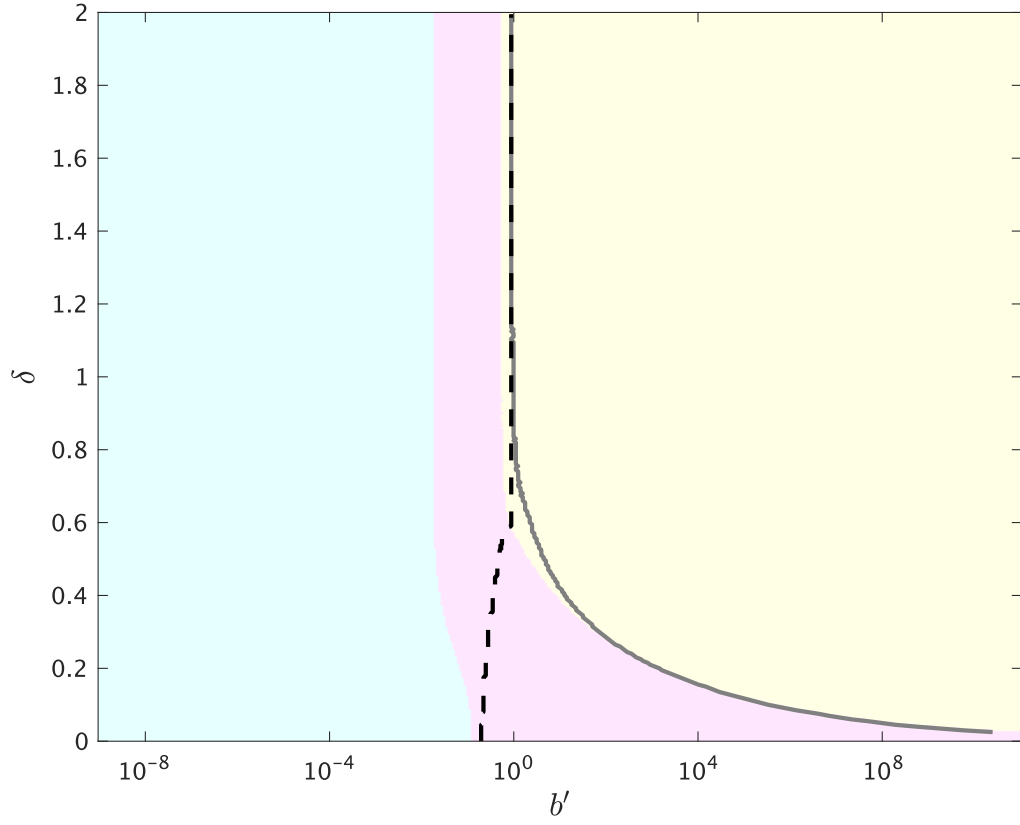


FIG. 8. Phase diagram of the indirect measurement with respect to the magnitude of the noise and degree of overlap between each signal. Semi-log plot of the peak positions of $\Lambda(b', 2; w_0)$ (black dashed and grey solid lines) with $w_0 = \{5, 10, \pm\delta\}$ as $K_0 = 2$. The inequality $\tilde{F}(b', 0; w_0) < \tilde{F}(b', 1; w_0)$ holds for $b' < b'_{\text{sn}}$ (region in light blue), $\tilde{F}(b', 0; w_0) > \tilde{F}(b', 1; w_0)$ holds for $b'_{\text{sn}} < b' < b'_{\text{ss}}$ (region in light pink), and $\tilde{F}(b', 1; w_0) > \tilde{F}(b', 2; w_0)$ holds for $b' > b'_{\text{ss}}$ (region in light yellow).

SUPPLEMENTARY NOTE 1: EXPLICIT EXPRESSION OF THE HAMILTONIAN

Here, we show a more explicit expression of Eq. (10):

$$H(w; w_0) = J(w_0, w_0) - 2J(w_0, w) + J(w, w) \quad (\text{S1})$$

with

$$J(w, w') := \sum_{j=1}^K \sum_{k=1}^{K'} a_j a'_k \sqrt{\frac{2}{\rho_j + \rho'_k}} \exp\left(-\frac{(\mu_j - \mu'_k)^2}{2(\rho_j^{-1} + \rho_k'^{-1})}\right) \tilde{J}(\rho_j, \mu_j, \rho'_k, \mu'_k) \quad (\text{S2})$$

for $w' := \{a'_k, \rho'_k, \mu'_k\}_{k=1}^{K'}$ as $KK' > 0$ and $J(w, w') := 0$ as $KK' = 0$, where

$$\tilde{J}(\rho_j, \mu_j, \rho'_k, \mu'_k) := \frac{\sqrt{\pi}}{2} \operatorname{erf}\left(\sqrt{\frac{\rho_j + \rho'_k}{2}} \left(x_n - \frac{\mu_j \rho_j + \mu'_k \rho'_k}{\rho_j + \rho'_k}\right)\right) - \frac{\sqrt{\pi}}{2} \operatorname{erf}\left(\sqrt{\frac{\rho_j + \rho'_k}{2}} \left(x_1 - \frac{\mu_j \rho_j + \mu'_k \rho'_k}{\rho_j + \rho'_k}\right)\right). \quad (\text{S3})$$

Note that $\tilde{J}(\rho_j, \mu_j, \rho'_k, \mu'_k) = \sqrt{\pi}$ holds for $x_1 \rightarrow -\infty$ and $x_n \rightarrow \infty$ as a Gaussian integral. We also define

$$\tilde{J}^2(\rho, \mu) := \tilde{J}(\rho, \mu, \rho, \mu) = \frac{\sqrt{\pi}}{2} \operatorname{erf}(\sqrt{\rho}(x_n - \mu)) - \frac{\sqrt{\pi}}{2} \operatorname{erf}(\sqrt{\rho}(x_1 - \mu)) \quad (\text{S4})$$

for convenience. Now, we obtain the average part of $\tilde{F}_n(b, K)$,

$$b' \tilde{F}(b', K; w_0) = \frac{b' J(w_0; w_0)}{2} - \log \int \exp\left(-\frac{b'}{2} \tilde{H}(w; w_0)\right) \varphi(w | K) dw \quad (\text{S5})$$

with $\tilde{H}(w; w_0) := J(w, w) - 2J(w_0, w)$, where $b' J(w_0; w_0)$ depends exclusively on a typical observation of D^n and not on the inference of w , especially at $b = b_0$.

In the case of $K_0 = 1$ as in Sec. IID, we obtain

$$b' J(w_0, w_0) = \frac{a^{*2} b}{\sqrt{\rho^*} \Delta x} \tilde{J}^2(\rho^*, \mu^*) \leq \frac{\sqrt{\pi} a^{*2} b}{\sqrt{\rho^*} \Delta x} \quad (\text{S6})$$

for $w_0 := \{a^*, \rho^*, \mu^*\}$, where the equality holds for $x_1 \rightarrow -\infty$ and $x_n \rightarrow \infty$. This means that the typical quality of D^n depends on the signal-to-noise ratio $a^* \sqrt{b_0}$, the signal-to-resolution ratio $(\sqrt{\rho^*} \Delta x)^{-1}$, and the measurement interval $[x_1, x_n]$.

In the case of $K_0 = 2$ as in Sec. IIE, we obtain

$$b' J(w_0, w_0) = \frac{a^{*2} b}{4\sqrt{\rho^*} \Delta x} \left(\tilde{J}^2(\rho^*, \mu_1^*) + \tilde{J}^2(\rho^*, \mu_2^*) + 2 \exp(-\delta^2 \rho^*) \tilde{J}^2(\rho^*, \mu_c) \right) \leq \frac{\sqrt{\pi} a^{*2} b}{2\sqrt{\rho^*} \Delta x} (1 + \exp(-\delta^2 \rho^*)) \quad (\text{S7})$$

especially for $w_0 := \{a_k^*, \rho_k^*, \mu_k^*\}_{k=1}^2$, $\delta := |\mu_1^* - \mu_2^*|/2 \geq 0$ and $\mu_c := (\mu_1^* + \mu_2^*)/2$ such that $a_1^* = a_2^* = a^*/2$, $\rho_1^* = \rho_2^* = \rho^*$, where the equality holds for $x_1 \rightarrow -\infty$ and $x_n \rightarrow \infty$. This means that the typical quality of D^n depends on the signal-to-noise ratio $a^* \sqrt{b_0}/2$, the signal-to-resolution ratio $(\sqrt{\rho^*} \Delta x)^{-1}$, the measurement interval $[x_1, x_n]$, and additionally the degree of overlap between each signal $\delta \sqrt{\rho^*}$. In Sec. IIF, we adopted δ as the degree of overlap between each signal, where ρ^* was fixed, since both $(\sqrt{\rho^*} \Delta x)^{-1}$ and $\delta \sqrt{\rho^*}$ depend on ρ^* . Note that the term $\exp(-\delta^2 \rho^*) \leq 1$ can be regarded as a perturbation, where Eq. (S7) is reduced to Eq. (S6) for $\delta = 0$ and $\mu_c = \mu^*$.

SUPPLEMENTARY NOTE 2: GENERAL DEFINITION OF THE BAYES SPECIFIC HEAT

Here, we derive Eq. (11) from a broader perspective of statistical inference beyond our setup. We start by introducing the conditional probability density

$$p(w | D^n, \beta, b, K) := \frac{1}{Z_n(\beta, b, K)} \exp\left(-\frac{n\beta}{2} L_n(w; b)\right) \varphi(w | K) \quad (\text{S8})$$

with $\beta \geq 0$ being the *inverse temperature* [38], the empirical log loss function

$$L_n(w; b) := -\frac{1}{n} \sum_{i=1}^n \log p(Y_i | x_i, w, b) \quad (\text{S9})$$

and the partition function

$$Z_n(\beta; b, K) := \int \exp\left(-\frac{n\beta}{2} L_n(w; b)\right) \varphi(w | K) dw. \quad (\text{S10})$$

Note that Eq. (S8) for $\beta = 1$ is just Bayes' theorem, where $p(w | D^n, 1, b, K)$ and $Z_n(1; b, K)$ are the posterior distribution and marginal likelihood, respectively. If $\beta \rightarrow \infty$ and $\varphi(\hat{w} | K) > 0$, then $p(w | D^n, \beta, b, K)$ converges to $\delta(w - \hat{w})$, where \hat{w} is the maximum likelihood estimator [38]. Notably, $p(w | D^n, \beta, b, K) = \varphi(\hat{w} | K)$ holds for $\beta = 0$.

Here, we define the specific heat

$$C_n(\beta; b, K) := \frac{\partial \langle nL_n(w; b) \rangle_\beta}{\partial \beta^{-1}} = \beta^2 I_n(\beta; b, K) \quad (\text{S11})$$

with the Fisher information

$$I_n(\beta; b, K) := \left\langle \left(\frac{\partial}{\partial \beta} \log p(w | D^n, \beta, b, K) \right)^2 \right\rangle_\beta = \langle (nL_n(w))^2 \rangle_\beta - \langle nL_n(w) \rangle_\beta^2, \quad (\text{S12})$$

where the average $\langle \cdots \rangle_\beta := \int (\cdots) p(w | D^n, \beta, b, K) dw$. Considering the connection between statistical inference and statistical physics, $\langle nL_n(w; b) \rangle_\beta$ is the internal energy for $nL_n(w; b)$ as the Hamiltonian of a disordered system and

$$F_n(\beta; b, K) := -\frac{1}{\beta} \log Z_n(\beta; b, K). \quad (\text{S13})$$

is the free energy. Then, we also obtain the relation

$$C_n(\beta; b, K) = -\beta^2 \frac{\partial^2 (\beta F_n)}{\partial \beta^2} \quad (\text{S14})$$

as in statistical physics. As the *Bayes* free energy is defined by $\tilde{F}_n(b, K) = F_n(1; b, K)$, we define the *Bayes* specific heat as $C_n(1; b, K)$, where this definition can be applied not only to $L_n(w; b)$ in our setup but also to any other empirical log loss functions without loss of generality. We should compare the *Bayes* specific heat, especially in the form of Eq. (S14), with the learning capacity [46], which is defined by the second derivative of the *Bayes* free energy with respect to n as an approximation of the second-order finite difference. Notably, these are different quantities, as β and n are different, while the quantities conditionally show similar asymptotic behaviours for $n \rightarrow \infty$. We show their similarities and differences in Supplementary note 3.

Now, we consider the specifics of our setup, i.e., the relation

$$L_n(w; b) = \frac{b}{2} E_n(w) - \frac{1}{2} \log \frac{b}{2\pi}. \quad (\text{S15})$$

Then, we obtain the scaling relations $C_n(\beta; b, K) = \tilde{C}_n(\beta', K)$ and $I_n(\beta; b, K) = \tilde{I}_n(\beta', K)$ for $\beta' := \beta b$, where the scaling functions are

$$\tilde{C}_n(\beta', K) := \frac{\partial \langle nE_n(w) \rangle_{\beta'}}{\partial \beta'^{-1}} = \beta'^2 \tilde{I}_n(\beta', K) \quad (\text{S16})$$

and

$$\tilde{I}_n(\beta', K) := \left\langle \left(\frac{\partial}{\partial \beta'} \log p(w | D^n, \beta, b, K) \right)^2 \right\rangle_{\beta'} = \langle (nE_n(w))^2 \rangle_{\beta'} - \langle nE_n(w) \rangle_{\beta'}^2. \quad (\text{S17})$$

Note that these scaling relations mean that the bivariate functions of (β, b) are exactly reduced to the univariate functions of β' , while $F_n(\beta; b, K)$ does not satisfy such a scaling relation, as shown by

$$F_n(\beta; b, K) = -\frac{1}{\beta} \log \int \exp\left(-\frac{n\beta'}{2} E_n(w)\right) \varphi(w | K) dw - \frac{n}{2} \log \frac{b}{2\pi}. \quad (\text{S18})$$

Now, we take $\beta = 1$, i.e. $\beta' = b$ and then obtain $\tilde{C}_n(b, K)$ in the form of Eq. (11) as the *Bayes* specific heat in our setup.

SUPPLEMENTARY NOTE 3: FINITE-SIZE SCALING

We show the derivation of Eq. (12), whose outline is mentioned in Sec. IVC, in more detail. We start from a broader perspective of statistical inference beyond our setup. The asymptotic behaviour of the free energy [38] is shown by

$$\beta F_n(\beta; b, K) = n\beta L_n(w'_0; b) + \lambda \log n\beta + (m-1) \log \log n\beta + O_p(\beta) \quad (\text{S19})$$

for $n \rightarrow \infty$, where w'_0 , $\lambda > 0$ and $m \geq 1$ are w that minimizes the Kullback-Leibler distance from $p(y_i | x_i, w_0, b_0)$ to $p(y_i | x_i, w, b)$, a rational number, called the real log canonical threshold, and a natural number, respectively. Note that $w'_0 = w_0$ holds if $b_0 = b$ and $K_0 = K$. By following Eq. (S14), we obtain

$$C_n(\beta; b, K) = \lambda - (m-1) \left(\frac{1}{\log n\beta} + \frac{1}{(\log n\beta)^2} \right) + o_p(\beta^2) \quad (\text{S20})$$

for $n \rightarrow \infty$. If we take $\beta \rightarrow \infty$, then $C_n(\beta; b, K) = \lambda + o_p(\beta^2)$ holds; the quantity $C_n(\beta; b, K)$ is not necessarily self-averaging. The relation $C_n(\beta; b, K) = \lambda$ holds for $n \rightarrow \infty$ with $\beta = O(1/\log n)$, which corresponds to the condition shown in Watanabe's corollary [41]; the quantity $C_n(\beta; b, K)$ is self-averaging under this condition. Here, we mention that the expectation of the learning capacity over the observation also converges to λ for $n \rightarrow \infty$ [46], while the definition of the learning capacity as a random variable is not suitable for this type of scaling analysis. This is a definite difference between the learning capacity and the *Bayes* specific heat.

Now, we consider the specifics of our setup, i.e., the relation

$$\tilde{C}_n(\beta', K) = \lambda - (m-1) \left(\frac{1}{\log n\beta'} + \frac{1}{(\log n\beta')^2} \right) + o_p(\beta'^2), \quad (\text{S21})$$

where the correspondence of (β, b) and β' is considered. Then, we obtain

$$\tilde{C}_n(b, K) = \lambda - (m-1) \left(\frac{1}{\log nb} + \frac{1}{(\log nb)^2} \right) + o_p(b^2) \quad (\text{S22})$$

for $\beta = 1$.

To evaluate the term $o_p(b^2)$ more tightly, we consider the additivity of statistical noise:

$$Y_i = f(x_i; w_0) + N_i, \quad (\text{S23})$$

where $N_i \sim \mathcal{N}(0, b_0^{-1})$. Then, we obtain

$$nE_n(w) = \sum_{i=1}^n s_i(w)^2 + 2 \sum_{i=1}^n s_i(w) N_i + b_0^{-1} R_n, \quad (\text{S24})$$

where $s_i(w) := f(x_i; w_0) - f(x_i; w)$ and $R_n := b_0 \sum_{i=1}^n N_i^2$. Following Eq. (11), we also obtain

$$\tilde{C}_n(b, K) = \left(\frac{b}{2}\right)^2 \left(\left\langle \left(\sum_{i=1}^n s_i(w)^2 \right)^2 \right\rangle - \left\langle \sum_{i=1}^n s_i(w)^2 \right\rangle^2 \right) + V_n(b, K) + \tilde{V}_n(b, K) + W_n(b, K) + \tilde{W}_n(b, K), \quad (\text{S25})$$

where

$$V_n(b, K) := b^2 \sum_{i \neq j} (\langle s_i(w) s_j(w) \rangle - \langle s_i(w) \rangle \langle s_j(w) \rangle) N_i N_j, \quad (\text{S26})$$

$$\tilde{V}_n(b, K) := b^2 \sum_{i=1}^n (\langle s_i(w)^2 \rangle - \langle s_i(w) \rangle^2) N_i^2, \quad (\text{S27})$$

$$W_n(b, K) := b^2 \sum_{i \neq j} (\langle s_i(w)^2 s_j(w) \rangle - \langle s_i(w)^2 \rangle \langle s_j(w) \rangle) N_j, \quad (\text{S28})$$

and

$$\tilde{W}_n(b, K) := b^2 \sum_{i=1}^n (\langle s_i(w)^3 \rangle - \langle s_i(w)^2 \rangle \langle s_i(w) \rangle) N_i. \quad (\text{S29})$$

We evaluate the order of each term in Eq. (S25) as $n \rightarrow \infty$. First, we obtain

$$\left(\frac{b}{2}\right)^2 \left(\left\langle \left(\sum_{i=1}^n s_i(w)^2 \right)^2 \right\rangle - \left\langle \sum_{i=1}^n s_i(w)^2 \right\rangle^2 \right) = \Lambda(b', K; w_0) \quad (\text{S30})$$

for $n \rightarrow \infty$ as a Riemann integral.

Second, we evaluate the order of $V_n(b, K)$ as $n \rightarrow \infty$. Now, we obtain

$$[V_n(b, K)] = 0 \quad (\text{S31})$$

for $n \rightarrow \infty$ such that

$$[(\langle s_i(w)s_j(w) \rangle - \langle s_i(w) \rangle \langle s_j(w) \rangle)] N_i N_j = (\langle s_i(w)s_j(w) \rangle - \langle s_i(w) \rangle \langle s_j(w) \rangle) [N_i][N_j] \quad (\text{S32})$$

is satisfied, where $[N_i] = 0$. Then, we also obtain

$$\begin{aligned} [V_n(b, K)^2] - [V_n(b, K)]^2 &= \frac{b^4}{b_0^2} \sum_{i \neq j} (\langle s_i(w)s_j(w) \rangle - \langle s_i(w) \rangle \langle s_j(w) \rangle)^2 \\ &= O\left(\frac{b^2}{b_0^2}\right) \end{aligned} \quad (\text{S33})$$

for $n \rightarrow \infty$ such that

$$\left[(\langle s_i(w)s_j(w) \rangle - \langle s_i(w) \rangle \langle s_j(w) \rangle)^2 N_i^2 N_j^2 \right] = (\langle s_i(w)s_j(w) \rangle - \langle s_i(w) \rangle \langle s_j(w) \rangle)^2 [N_i^2][N_j^2] \quad (\text{S34})$$

and

$$\begin{aligned} &[(\langle s_i(w)s_j(w) \rangle - \langle s_i(w) \rangle \langle s_j(w) \rangle) (\langle s_k(w)s_l(w) \rangle - \langle s_k(w) \rangle \langle s_l(w) \rangle)] N_i N_j N_k N_l \\ &= (\langle s_i(w)s_j(w) \rangle - \langle s_i(w) \rangle \langle s_j(w) \rangle) (\langle s_k(w)s_l(w) \rangle - \langle s_k(w) \rangle \langle s_l(w) \rangle) [N_i][N_j][N_k][N_l] \end{aligned} \quad (\text{S35})$$

are satisfied, where $[N_i] = 0$, $[N_i^2] = b_0^{-1}$, $\langle s_i(w) \rangle = O((nb)^{-1})$ and $\langle s_i(w)s_j(w) \rangle = O((nb)^{-1})$. In summary, we obtain

$$\begin{aligned} V_n(b, K) &= [V_n(b, K)] + O_p\left(\frac{b}{b_0}\right) \\ &= O_p\left(\frac{b}{b_0}\right) \end{aligned} \quad (\text{S36})$$

for $n \rightarrow \infty$.

In the same way, we also obtain

$$\tilde{V}_n(b, K) = [\tilde{V}_n(b, K)] + O_p\left(\frac{b}{\sqrt{nb_0}}\right) \quad (\text{S37})$$

with

$$\begin{aligned} [\tilde{V}_n(b, K)] &= \frac{b^2}{b_0} \sum_{i=1}^n (\langle s_i(w)^2 \rangle - \langle s_i(w) \rangle^2) \\ &= O\left(\frac{b}{b_0}\right), \end{aligned} \quad (\text{S38})$$

where $[N_i^2] = b_0^{-1}$, $[N_i^4] = 3/b_0^2$, $\langle s_i(w) \rangle = O((nb)^{-1})$ and $\langle s_i(w)^2 \rangle = O((nb)^{-1})$. This means that \tilde{V}_n is self-averaging; i.e., $\tilde{V}_n = [\tilde{V}_n] \geq 0$ holds for $n \rightarrow \infty$. Furthermore, we also obtain

$$W_n(b, K) = O_p\left(\frac{1}{n\sqrt{b_0}}\right), \quad (\text{S39})$$

and

$$\tilde{W}_n(b, K) = O_p \left(\frac{1}{n^{3/2} \sqrt{b_0}} \right) \quad (\text{S40})$$

for $n \rightarrow \infty$, where $[N_i] = 0$, $[N_i^2] = b_0^{-1}$, $[W_n] = 0$, $[\tilde{W}_n] = 0$, $\langle s_i(w) \rangle = O((nb)^{-1})$, $\langle s_i(w)^2 \rangle = O((nb)^{-1})$, $\langle s_i(w)^2 s_j(w) \rangle = O((nb)^{-2})$, and $\langle s_i(w)^3 \rangle = O((nb)^{-2})$. By considering the consistency between Eq. (S22) and Eq. (S25) with Eq. (S30) and Eqs. (S36 -S40), we obtain Eq. (12), where $\Lambda(b', K; w_0) = \lambda$ is a real log canonical threshold.

Here, we demonstrate the validity of Eq. (12). By performing the same simulation in Figs. 2 and 5 based on 100 different realizations of D^n , for $n = 101$, taken from identical $p(y_i | x_i, w_0, b_0)$, we calculated $\tilde{C}_n(b, K)$ for each realization. Phenomenologically, the expectation of $\tilde{C}_n(b, K)$ over the realizations is fairly consistent with $\Lambda(b', K; w_0)$ at any b when $K = 1$ for $(b_0, K_0) = (b_2, 1)$ (Fig. S1 a), when $K = 1$ for $K_0 = 2$ (Fig. S1 c), and when $K = 2$ for $(b_0, K_0) = (b_3, 2)$, where the standard deviations of $\tilde{C}_n(b, K)$ for the realizations is small enough (Fig. S2); the quantity $\tilde{C}_n(b, K)$ is considered to be self-averaging at any b in these cases without the condition $b = O(b_0/\log n)$. According to Eq. (12), these cases means that the expectation of $\tilde{C}_n(b, K)$ corresponds to the average term $\Lambda(b', K; w_0)$, where the standard deviation of $\tilde{C}_n(b, K)$ corresponds to the fluctuation term of order $O_p(\max((\log nb)^{-1}, b/b_0, (n\sqrt{b_0})^{-1}))$. Note that the standard deviation of $\tilde{C}_n(b, K)$ as the fluctuation term shows a dependence on $\Lambda(b', K; w_0)$ (Fig. S2), which is not predicted by Eq. (12).

In other cases, the expectation of $\tilde{C}_n(b, K)$ is not consistent with $\Lambda(b', K; w_0)$ at $b \gtrsim b_0$ (Fig. S1); finite-size effects on $\tilde{C}_n(b, K)$ appear at $b \gtrsim b_0$, where the term of order $O_p(b/b_0)$ is dominant. According to Eq. (S25) with Eqs. (S36 - S40), the expectation of $\tilde{C}_n(b, K)$ corresponds to $\Lambda(b', K; w_0) + \tilde{V}_n(b, K)$ as $n \rightarrow \infty$, where the standard deviation of $\tilde{C}_n(b, K)$ corresponds to $V_n(b, K) + W_n(b, K) + \tilde{W}_n(b, K)$ as $n \rightarrow \infty$. Phenomenologically, the expectations and standard deviations of $\tilde{C}_n(b, K)$ are roughly proportional to \sqrt{b} if b is large enough (Fig. S3) and also show a rough dependence on b_0^2 . We conjecture the relation

$$\tilde{C}_n(b, K) = \Lambda(b', K; w_0) + O_p \left(\frac{\sqrt{b}}{b_0^2} \right) \quad (\text{S41})$$

for $n, b \rightarrow \infty$ in these cases, i.e., a special case of Eq. (12). Note that $\tilde{C}_n(b, K)$ is considered to be self-averaging for $b = O(b_0/\log n)$ in all cases.

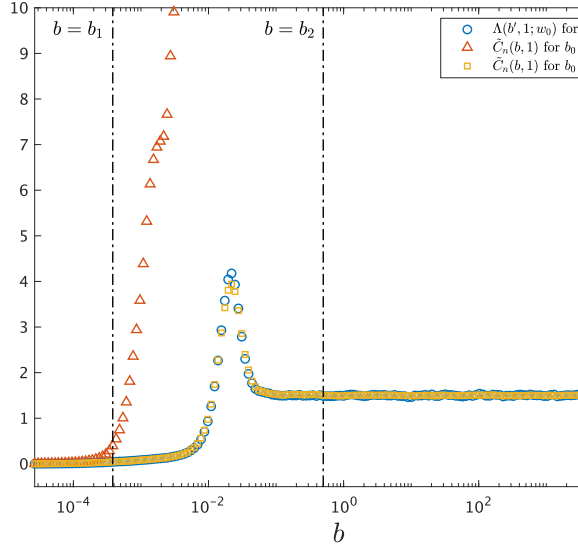
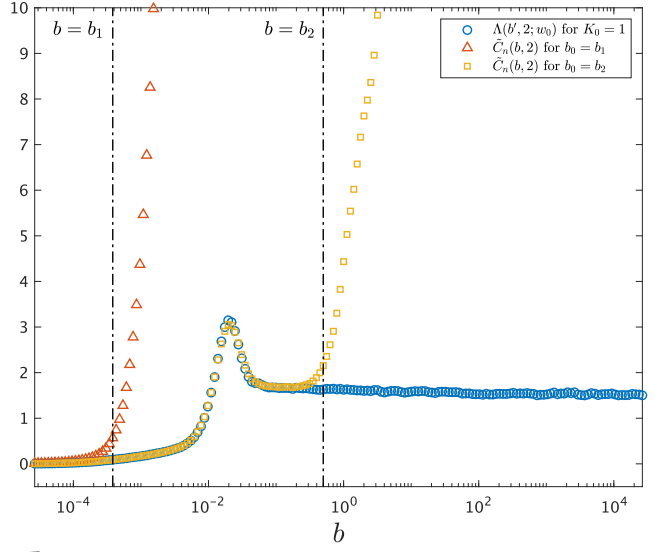
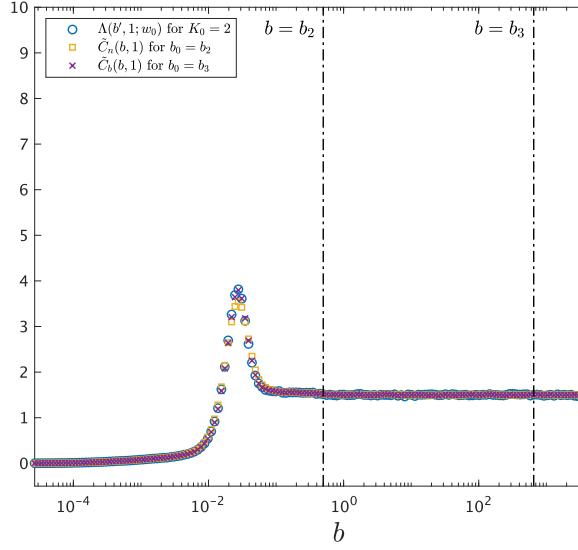
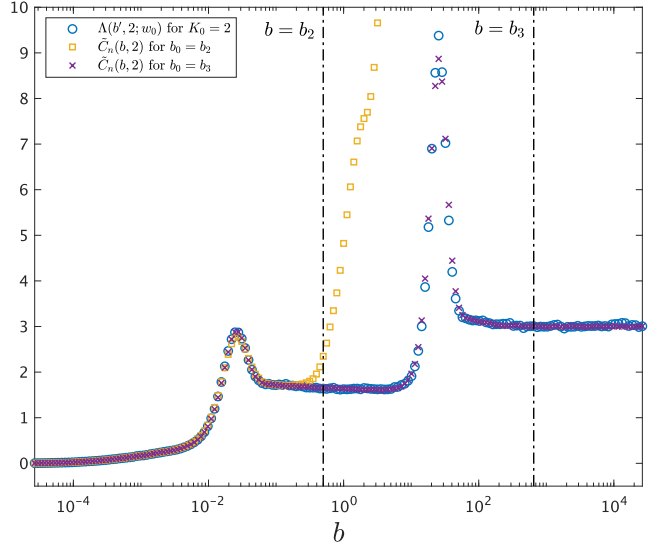
a**b****c****d**

FIG. S1 . Finite-size effects on the Bayes specific heat. Semi-log plots of $\Lambda(b', K; w_0)$ (blue circles) and the expectations of $\tilde{C}_n(b, K)$ over the realization of D^n for $b_0 = b_1$ (red triangles), $b_0 = b_2$ (yellow squares) and $b_0 = b_3$ (purple crosses) when (a) $K = 1$ and (b) $K = 2$, in the same case of Fig. 2, and when (c) $K = 1$ and (d) $K = 2$, in the same case of Fig. 5. Note that $\Lambda(b', K; w_0)$ is replotted from Figs. 3b and 6b, where $b = b' \Delta x$ ($b_1 := b'_1 \Delta x$, $b_2 := b'_2 \Delta x$, and $b_3 := b'_3 \Delta x$).

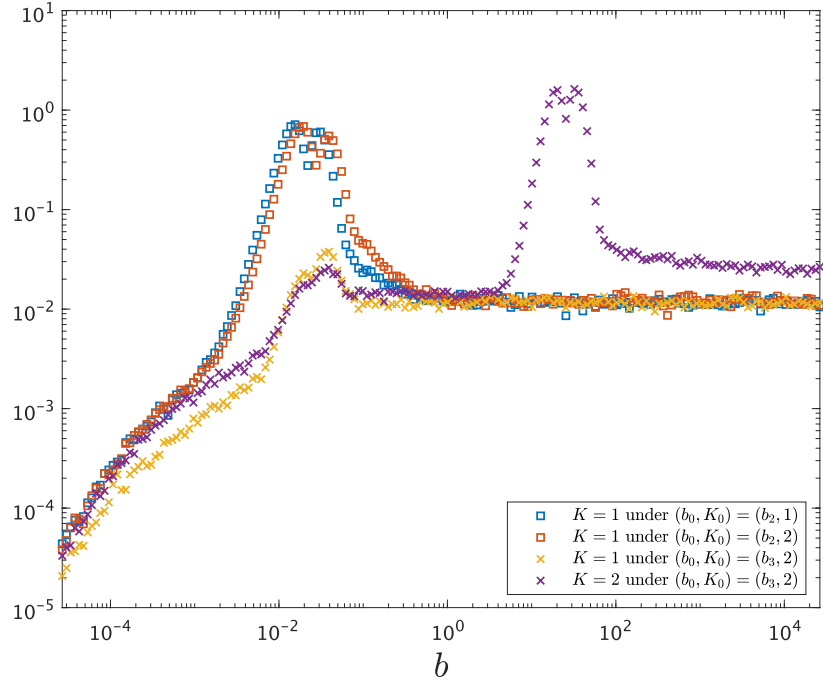


FIG. S2 . Fluctuation of the Bayes specific heat for the realizations. Log-log plots of the standard deviation of $\tilde{C}_n(b, K)$ for realizations of D^n for $(b_0, K_0) = (b_2, 1)$ (blue squares for $K = 1$), $(b_0, K_0) = (b_2, 2)$ (red squares for $K = 1$), and $(b_0, K_0) = (b_3, 2)$ (yellow crosses for $K = 1$ and purple crosses for $K = 2$), where each case corresponds to Fig. S1 .

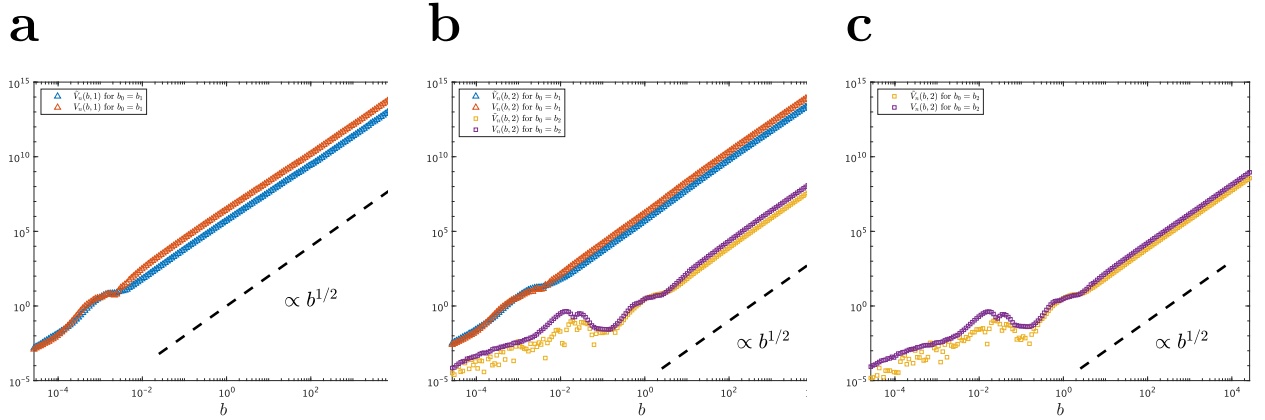


FIG. S3 . Scaling analyses of the Bayes specific heat. Log-log plots of the expectations (blue triangles for $K_0 = 1$ and yellow squares for $K_0 = 2$) of $\tilde{C}_n(b, K)$, subtracting $\Lambda(b', K; w_0)$ as the baseline, and the standard deviations (red triangles for $K_0 = 1$ and yellow squares for $K_0 = 2$) of $\tilde{C}_n(b, K)$ over the realization of D^n in the cases of (a) Fig. S1 a, (b) Fig. S1 b and (c) Fig. S1 d.